# UWB Communication Characteristics for Different Materials and Shapes of the Stairs

Chien-Ching Chiu
Tamkang University / Department of Electrical Engineering, Tamsui, Taiwan
Email: chiu@ee.tku.edu.tw

Yang-Ta Kao
Chihlee Institute of Technology / Department of Information Network Technology, Banciao, Taiwan
Email: ydkao@mail.chihlee.edu.tw

Shu-Han Liao and Yu-Fen Huang
Tamkang University / Department of Electrical Engineering, Tamsui, Taiwan
Email: bb0918@hotmail.com, sai27candace@yahoo.com.tw

***Abstract*—A comparison of ultra-wideband (UWB) communication characteristics for two different shapes of stairs with concrete and iron materials are investigated. The impulse responses of these stairs are computed by shooting and bouncing ray/image (SBR/Image) techniques and inverse Fourier transform. Numerical results show that the bit error rate (BER) of binary-pulse amplitude modulation (B-PAM) system for the concrete case is smaller than that for the iron case. Finally, it is worth noting that in these cases the present work provides not only comparative information but also quantitative information on the performance reduction.**

***Index Terms*—UWB, SBR/Image, BER, B-PAM**

## I. INTRODUCTION

Ultra-wideband (UWB) technology is an ideal candidate for a low power, low cost, high data rate, and short range wireless communication systems. According to the Federal Communication Commission (FCC), UWB signal is defined as a signal having fractional bandwidth greater than 20% of the center frequency [1]. Ultra wide bandwidth of the system causes antenna design to be a new challenge [2]-[5]. This is because the multi-path fading and interferences become more apparent than in narrow band system. In order to overcome this phenomenon, smart antenna technologies are envisaged as one of possible solutions.

The analysis and design of an UWB communication system require an accurate channel model to determine the maximum achievable data rate, to design efficient modulation schemes, and to study associated signal-processing algorithms [5]. Besides, a prior knowledge of the characteristics of the channel is necessary for understanding how is the signal affected in the environment. Therefore, many techniques of channel calculation have been developed in recent years. Especially, using Ray-Tracing method to obtain impulse response is extensively applied [6]-[8]. In indoor radio wave propagation, different environments have different channel effects, and channel characteristics determine the range of cover power and the maximum transmission rate of the system. It is important to know the parameters of the indoor radio environment between the statistical properties. Note that the conductivity and dielectric constant of materials will change with the frequency in the UWB channel. As a result, different frequencies of the same materials will have different propagation characteristics. Therefore, the frequency dependence of the dielectric and conductivity of materials is used in the channel simulation [9].

This paper aims at using shooting and bouncing ray/image (SBR/Image) method to calculate two different UWB stairs, and further compares their channel characteristics. The effects of different materials with concrete and iron on the UWB communication characteristics are presented. The frequency dependence for dielectric constant and the conductivity of materials change is carefully considered. In section II, the channel modeling and system description are presented. In section III, we show the numerical results. Finally, the conclusion is drawn in section Ⅳ.

## II. CHANNEL MODELING AND SYSTEM DESCRIPTION

### A. Channel Modeling

The following two steps are used to calculate the multi-path radio channel.

(1)Frequency responses for sinusoidal waves by SBR/Image techniques

Manuscript received February 15, 2011; revised May 15, 2011; accepted September 30, 2011.

corresponding author: Chien-Ching Chiu


doi:10.4304/jcm.6.8.628-632

The SBR/Image method can deal with high frequency radio wave propagations in the complex indoor environments [10], [11]. It conceptually assumes that many triangular ray tubes are shot from the transmitting antenna (TX), and each ray tube, bouncing and penetrating in the environments is traced in the indoor multi-path channel. If the receiving antenna (RX) is within a ray tube, the ray tube will have contributions to the received field at the RX, and the corresponding equivalent source (image) can be determined. By summing all contributions of these images, we can obtain the total received field at the RX. The depolarization yielded by multiple reflections on walls and floors is also taken into account in our simulations. Note that the different values of dielectric constant and conductivity of materials for different frequency are carefully considered in channel modeling.

(2) Inverse Fast Fourier Transform (IFFT) and Hermitian Processing

The frequency responses are transformed to the time domain by using the inverse Fourier transform with the Hermitian signal processing [12]. By using the Hermitian processing, the pass-band signal is obtained with zero padding from the lowest frequency down to direct current (DC), taking the conjugate of the signal, and reflecting it to the negative frequencies. The result is then transformed to the time domain using IFFT [13]. Since the signal spectrum is symmetric around DC. The resulting doubled-side spectrum corresponds to a real signal in the time domain.

The equation for modeling the multi-path radio channel is a linear filter with an impulse response given by

$$h(t)=\sum_{n=1}^{N}\alpha_n\delta(t-\tau_n) \tag{1}$$

where *N* is the number of paths observed at time. $\delta(\ )$ is the Dirac delta function. $a_n$ and $\tau_n$ are the channel gain and time delay for the *n*-th path respectively.

*B. System Block Diagram*

Block diagram of the simulated communication system is shown in Fig.1.The transmitted UWB pulse stream can be expressed as the following [14]:

$$x(t)=\sum_{n=1}^{\infty} p[t-(n-1)T_d]d_n \tag{2}$$

where $p(t)$ is the transmitted waveform. $d_n\in\{\pm 1\}$ is a binary-pulse amplitude modulation (B-PAM) symbol and is assumed to be independent identically distributed (i.i.d.). $T_d$ is the duration of the transmitting signal. The transmitted waveform $p(t)$ is the Gaussian waveform with ultra-short duration $T_p$ at the nanosecond scale. Note that $T_d$ is the duration of the transmitting signal and

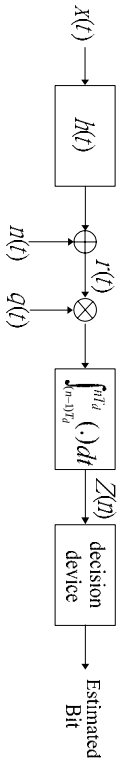


Figure 1. Block diagram of the simulated communication system.

$T_p$ is the pulse duration. The value of $T_d$ is usually much larger than that of $T_p$. The Gaussian waveform $p(t)$ can be described by the following expression:

$$p(t)=\frac{1}{\sqrt{2\pi}\sigma}e^{\frac{-t^2}{2\sigma^2}} \tag{3}$$

where $t$ and $\sigma$ are time and standard deviation of the Gaussian wave, respectively. The average transmit energy symbol $E_t$ can be expressed as

$$E_t=\int_0^{T_d} p^2(t)dt \tag{4}$$

The received signal *r*(*t*) can be expressed as follows:

$$r(t)=\left[x(t)\otimes h(t)\right]+n(t) \tag{5}$$

where *x*(*t*) is the transmitted signal and $h(t)$ is the impulse response of the equivalent baseband, *n*(*t*) is the white Gaussian noise with zero mean and variance $N_0/2$. The correlation receiver samples the received signal at the symbol rate and correlates them with suitably delayed references given by

$$q(t)=p[t-\tau_1-(n-1)T_d] \tag{6}$$

where $\tau_1$ is the delay time of the first wave. The output of the correlator at $t = nTd$ is [15], [16]

$$Z(n) = \int_{(n-1)T_d}^{nT_d} \left\{ \left[ \sum_{n=1}^{\infty} p[t-(n-1)T_d]d_n \right] \otimes h(t) \right\} \cdot q(t)\,dt + \int_{(n-1)T_d}^{nT_d} n(t)q(t)\,dt \quad (7)$$
$$= V(n) + \eta(n)$$

It can be shown that the noise components $\eta(n)$ of Eq. (7) are uncorrelated Gaussian random variables with zero mean. The variance of the output noise $\eta$ is

$$\sigma^2 = \frac{N_0}{2} E_t \quad (8)$$

The conditional error probability of the *n*-th bit is thus expressed by:

$$P_e\left[Z(n) \mid \vec{d}\right] = \frac{1}{2} erfc\left[\frac{V(n)}{\sqrt{2}\sigma} \cdot (d_n)\right] \quad (9)$$

where $erfc(x) = \frac{2}{\sqrt{\pi}} \int_x^{\infty} e^{-y^2} dy$ is complementary error function and $\left\{\vec{d}\right\} = \{d_0, d_1, \ldots, d_n\}$ is the binary sequence. Note that the average bit error rate (BER) for B-PAM impulse radio UWB system can be expressed as [17]

$$BER = \sum_{i=1}^{2^n} P(\vec{d}) \cdot \frac{1}{2} erfc\left[\frac{V(i)}{\sqrt{2}\sigma} \cdot (d_n)\right] \quad (10)$$

where $P(\vec{d})$ is the occurring probability of the binary sequence $\vec{d}$.

## III. Numerical Results

This paper intends to compare the channel characteristics of two different stairs. A two story building is considered in the paper. The length is five meters, the width is three meters, and the height is six meters. Fig. 2(a) and Fig. 2(b) are the side view of projection the building in x-z plane and y-z plane, respectively. The material of the wall is concrete, and the clapboard between the floors is also concrete, and the thick is 0.1 meters. The stairs are in the middle of the building.

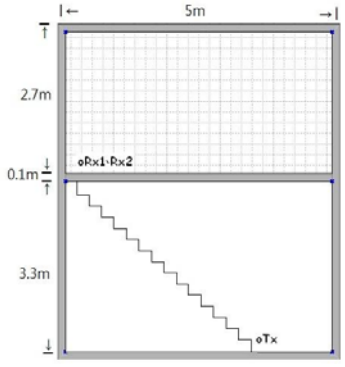


Figure 2(a). Indoor environment with dimensions of 5m (Length) x 3m (wide).x 6m (Height). Tx denotes the transmitter. Rx1 and Rx2 are the receivers. (a) projection in the x-z plane.

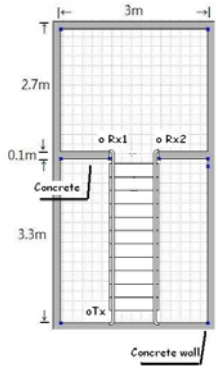


Figure 2(b). Indoor environment with dimensions of 5m (Length) x 3m (wide).x 6m (Height). Tx denotes the transmitter. Rx1 and Rx2 are the receivers. (b) projection in the y-z plane.

These are two different materials of stairs considered in the simulation. One material is concrete and the other is iron. For the material of concrete cases, all stairs are concrete except that the top of steps are wooden boards, as shown in Fig. 3(a). For the material of iron case, it is all made of iron, as shown in Fig. 3(b). In the simulation, all walls are made of concrete which the thick is 50 centimeters.

Note that the conductivity and dielectric constant of materials will change with the frequency in the UWB channel. As a result, different frequencies of the same materials will have different propagation characteristics.

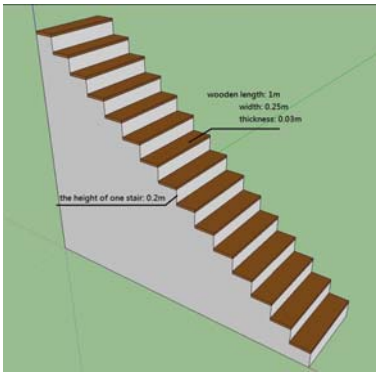


Figure 3(a). Various three-dimensional shape stairs. (a) the concrete stairs.

Therefore, the frequency dependence of the dielectric and

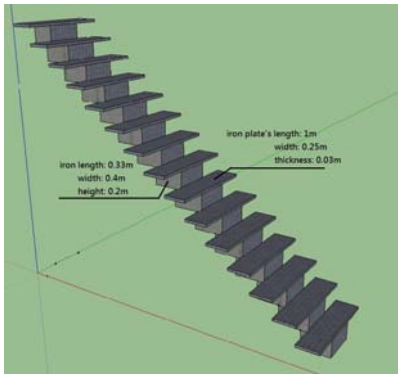


Figure 3(b). Various three-dimensional shape stairs. (b) the iron stairs

conductivity of materials is carefully considered in the channel simulation [18].

The transmitting and receiving antennas are both short dipole antennas and vertically polarized. The transmitting antenna is located at Tx (3.8, 1, 1)m with the fixed height 1 meter. There are 24 and 39 receiving points on the ground and the first floor respectively. The locations of receiving antennas are distributed uniformly with a fixed height of 1m. The distance between two adjacent receiving points is 0.5m. The maximum number of bounces is set to be five in the simulation and the convergence is confirmed.

The impulse response of concrete stairs and iron stairs at Rx1(0.5,0.5,4.3)m are shown in Fig. 4(a) and Fig. 4(b) respectively.

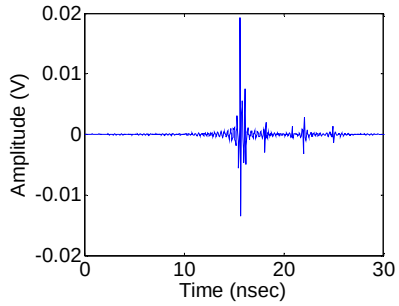


Figure 4(a). Impulse response of different stairs. (a) the concrete stairs.

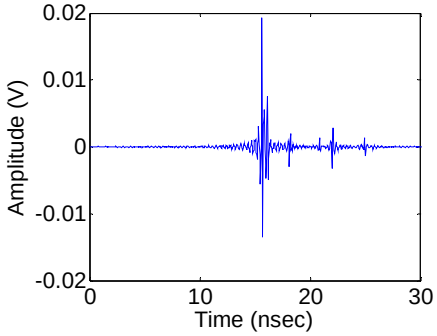


Figure 4(b). Impulse response of different stairs. (b) the iron stairs.

Next, let us consider the BER performance for these stairs. Here SNR is defined as the ratio of the average power to the noise power at the front end of the receiver. It is shown in Fig. 5, the BER to SNR of the receiver Rx2 for two different stairs. It is shown that the BER of the iron stairs is higher than the concrete stairs. This is due to the fact that the reflection coefficient of the iron is larger than that of the concrete, and the multi-path effect for the iron stairs is more severe. The calculated BER are used to compute the outage probability. The BER at 100M bps and SNR (signal to noise ratio) = 20dB are computed. For the BER requirement of BER < $10^{-3}$, the outage probabilities for the stairs of concrete and iron cases are presented. These are 63 received points uniformly distributed in the environment with a distance of 0.5m. Fig. 6 is the outage probabilities for the concrete stairs and the iron stairs in the indoor environment. At 100M bps transmission rate and for a BER < $10^{-3}$, it is seen that the outage probabilities at SNR=16dB are about 8% and 12% for the materials of concrete stairs and iron stairs respectively. This situation can be explained by the fact that the multi-path effect for the iron cases is very severe due to the total reflection. As a result, the performance of outage probability with iron stairs is worse than concrete stairs in UWB environment. Finally, it is worth noting that in these cases the present work provides not only comparative information but also quantitative information on the performance reduction.

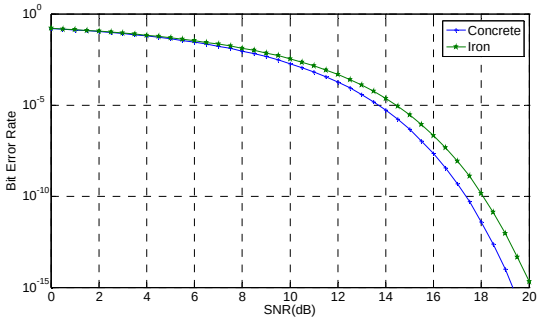


Figure 5(a). BER versus SNR for the different materials of stairs at Rx2.

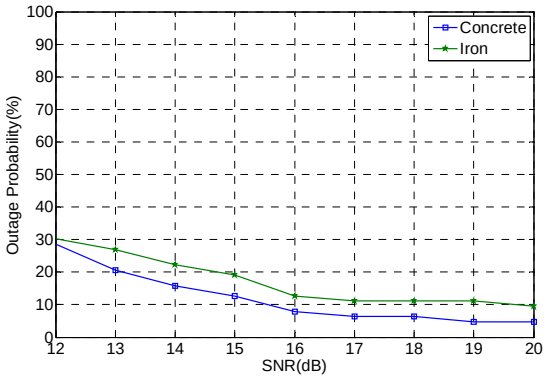


Figure 5(b). Outage probability versus SNR for the different materials of stairs.

## IV. Conclusion

A comparison of UWB communication characteristics for different materials and shapes of the stairs are presented. By using the impulse response of the multi-path channel, the BER for high-speed UWB indoor communication has been calculated. The frequency dependence of materials utilized in the structure on the indoor channel is accounted for in the channel simulation. i.e., the dielectric constant and conductivity of obstacles are not assumed to be frequency independent. The outage probabilities for 100M bps B-PAM and for a BER <10-3 versus SNR are calculated. The performance of outage probability for iron stairs is worse than that for concrete stairs in UWB environment. This is due to the multi-path effect is severe when iron stairs exist in the room. Finally, it is worth noting that in these cases the present work provides not only comparative information but also quantitative information on the performance reduction.

## REFERENCES


[1] M. H. Ho, S. H. Liao and C. C. Chiu, "UWB Communication Characteristics for Different Distribution of People and Various Materials of Walls," *Tamkang Journal of Science and Engineering* Vol. 13, No.3 , pp.315-326 Sep. 2010.

[2] C. L. Liu, M. H. Ho, C. C. Chiu and C. Y. Cheng, "A Comparison of UWB Communication Characteristics for Various Corridors." ACTA International Journal of Modelling and Simulation Vol. 30, No. 2 pp. 172-177, May. 2010.

[3] S. H. Liao, M. H. Ho and C. C. Chiu "Bit Error Rate Reduction for Multiusers by Smart UWB Antenna Array.", Progress In Electromagnetic Research C Vol. 16. PIER C 16, pp. 85-98, Sep. 2010.

[4] M. H. Ho, S. H. Liao and C. C. Chiu, "A Novel Smart UWB Antenna Array Design by PSO," Progress In Electromagnetic Research C Vol. 15. PIER C 15, pp. 103-115, Aug. 2010.

[5] Z. Irahhauten, H. Nikookar, and G.J.M. Janssen, "An overview of ultra wide band indoor channel measurements and modeling," *IEEE Microwave and Wireless Components Letters, see also IEEE Microwave and Guided Wave Letters*, Vol. 14, pp. 386 -388, Aug. 2004.

[6] G. Liang and H. L. Bertoni, "A new approach to 3-D ray tracing for propagation prediction in cities," *IEEE Trans. Antennas Propagat*., Vol. 46, pp. 853-863, June 1998.

[7] Y. Zhang, "Ultra-Wide Bandwidth Channel Analysis In Time Domain Using 3-D Ray Tracing," *High Frequency Postgraduate Student Colloquium of IEEE*, pp. 6-7, Sep. 2004.

[8] S. Woo, H. Yang, M. Park, and B. Kang, "Phase-Included Simulation of UWB channel, "*IEICE Trans. Commum*., Vol. E88-B, pp.1294-1297, March 2005.

[9] A.S. Jazi, S.M. Riad, A. Muqaibel, and A. Bayram, "Through the Wall Propagation and Material Characterization," *DARPA NETEX Program Report*, Nov. 2002.

[10] S. H. Liao, H. P. Chen, C. C. Chiu, and C. L. Liu "Channel Capacities of Indoor MIMO-UWB Transmission for Different Material Partitions.", Tamkang Journal of Science and Engineering Vol. 14, No.1, pp. 49-63, Mar. 2011.

[11] S. H. Liao, C. C. Chiu, M. H. Ho and C. L. Liu "Channel Capacity of Multiple-Input Multiple-Output Ultra Wide Band Systems with Single Co-channel Interference.", International Journal of Communication Systems, Vol. 23, Issue 12, pp. 1600-1612, Dec 2010.

[12] I. Oppermann, M. Hamalainen, and J. Iinatti, UWB Theory and Applications (John Wiley & Sons, 2004).

[13] E. W. Kamen and B. S. Heck, Fundamentals of Signals and Systems Using the Web and Matlab (Prentice-Hall, 2000).

[14] Zhi Tian and G. B. Giannakis, "BER sensitivity to mistiming in ultra-wideband impulse Radios-part I: nonrandom channels," *IEEE Transactions on Signal Processing*, pp. 1550 - 1560, Apr 2005.

[15] E. A. Homier and R. A. Scholtz, "Rapid acquisition of ultra-wideband signals in the dense multipath channel," *IEEE Conference in Ultra Wideband System and Technologies*, pp. 105 – 109, 2002.

[16] D. J. Gargin, "A fast and reliable acquisition scheme for detecting ultra wide-band impulse radio signals in the presence of multi-path and multiple access interference" *2004 International Workshop on Ultra Wideband System*, pp. 106 – 110, May 2004.

[17] C. L. Liu, C. C. Chiu, S. H. Liao and Y. S. Chen, "Impact of Metallic Furniture on UWB Channel Statistical Characteristics," *Tamkang Journal of Science and Engineering*, vol. 12, No.3, pp. 271-278, Sept. 2009.

[18] A. S. Jazi, S. M. Riad, A. Muqaibel, and A. Bayram, Through the Wall Propagation and Material Characterization, *DARPA NETEX Program Report*, 2002.


**Chien-Ching Chiu** received his BSCE degree from National Chiao Tung University, Hsinchu, Taiwan, in 1985 and his MSEE and PhD degrees from National Taiwan University, Taipei, in 1987 and 1991, respectively.

From 1987 to 1989, he was a communication officer with the ROC Army Force. In 1992 he joined the faculty of the Department of Electrical Engineering, Tamkang University, where he is now a professor. From 1998 to 1999, he was a visiting scholar at the Massachusetts Institute of Technology, Cambridge, and the University of Illinois at Urbana-Champaign. He is a visiting professor with the University of Wollongong, Australia, in 2006. Moreover, he was a visiting professor with the University of London, United Kingdom, in 2011.

His current research interests include microwave imaging, numerical techniques in electromagnetics, indoor wireless communications, and ultrawideband communication systems. He has published more than 90 journal papers on inverse scattering problems, communication systems and optimization algorithms.

**Yang-Ta Kao** received the B.S. degree in information engineering from Tamkang University, Taipei, Taiwan in 1996, the M.S. degree in computer science and information engineering from National Chiao Tung University, Hsinchu, Taiwan in 1998 and the Ph.D. degrees in information engineering from Tamkang University, Taipei, Taiwan in 2006. He is currently the chief of Department of Information Network Technology, Chihlee Institute of Technology. His current research interests include pattern recognition and image processing.

**Shu-Han Liao** was born in Taipei, Taiwan, Republic of China, on September 18, 1982. He received the M.S.C.E. degree from Feng Chia University in 2008, and now is working toward Ph.D degrees in the Department of Electrical Engineering, Tamkang University. His current research interests include indoor wireless communication systems, ultra-wideband systems, and MIMO systems.

**Yu-Fen Huang** was born in Taipei, Taiwan, Republic of China in 1989. She received the B.S. degree in Electrical Engineering from TamKang University in 2011, and now is working toward M.S. degrees in the Department of Communications Engineering, Yuan Ze University. Her current research interests include structure and applications of Golay complementary sequences.